the FEBS Journal

Site-directed mutagenesis of selected residues at the active site of aryl-alcohol oxidase, an H_2O_2-producing ligninolytic enzyme

Patricia Ferreira[1,*], Francisco J. Ruiz-Dueñas[1], María J. Martínez[1], Willem J. H. van Berkel[2] and Angel T. Martínez[1]

1 Centro de Investigaciones Biológicas, CSIC, Madrid, Spain
2 Laboratory of Biochemistry, Wageningen University, Wageningen, the Netherlands

Keywords
aryl-alcohol oxidase (EC 1.1.3.7); flavoenzyme; molecular docking; site-directed mutagenesis; substrate-binding site

Correspondence
A. T. Martínez, Centro de Investigaciones Biológicas, CSIC, Ramiro de Maeztu 9, E-28040 Madrid, Spain
Fax: +34 915360432
Tel: +34 918373112
E-mail: ATMartinez@cib.csic.es

***Present address**
Department of Biochemistry and Molecular Biology, College of Medicine, Drexel University, Philadelphia, PA, USA

(Received 17 July 2006, revised 26 August 2006, accepted 1 September 2006)

doi:10.1111/j.1742-4658.2006.05488.x

Aryl-alcohol oxidase provides H_2O_2 for lignin biodegradation, a key process for carbon recycling in land ecosystems that is also of great biotechnological interest. However, little is known of the structural determinants of the catalytic activity of this fungal flavoenzyme, which oxidizes a variety of polyunsaturated alcohols. Different alcohol substrates were docked on the aryl-alcohol oxidase molecular structure, and six amino acid residues surrounding the putative substrate-binding site were chosen for site-directed mutagenesis modification. Several *Pleurotus eryngii* aryl-alcohol oxidase variants were purified to homogeneity after heterologous expression in *Emericella nidulans*, and characterized in terms of their steady-state kinetic properties. Two histidine residues (His502 and His546) are strictly required for aryl-alcohol oxidase catalysis, as shown by the lack of activity of different variants. This fact, together with their location near the isoalloxazine ring of FAD, suggested a contribution to catalysis by alcohol activation, enabling its oxidation by flavin-adenine dinucleotide (FAD). The presence of two aromatic residues (at positions 92 and 501) is also required, as shown by the conserved activity of the Y92F and F501Y enzyme variants and the strongly impaired activity of Y92A and F501A. By contrast, a third aromatic residue (Tyr78) does not seem to be involved in catalysis. The kinetic and spectral properties of the Phe501 variants suggested that this residue could affect the FAD environment, modulating the catalytic rate of the enzyme. Finaly, L315 affects the enzyme k_{cat}, although it is not located in the near vicinity of the cofactor. The present study provides the first evidence for the role of aryl-alcohol oxidase active site residues.

Lignin degradation is a key process for carbon recycling in forests and other land ecosystems, as well for industrial utilization of lignocellulosic materials (e.g. in paper manufacture or ethanol production). The process has been defined as an enzymatic combustion where lignin aromatic units are oxidized by hydrogen peroxide generated by extracellular oxidases in a reaction catalyzed by high-redox-potential peroxidases [1]. Several oxidases have been reported as being potentially involved in hydrogen peroxide generation by ligninolytic fungi. However, some of them can be discounted because of their intracellular location, and only extracellular glyoxal oxidase, pyranose-2-oxidase and aryl-alcohol oxidase (AAO) are currently considered to be involved in lignin biodegradation. The model basidiomycete *Phanerochaete chrysosporium* produces the two former enzymes [2,3]. In contrast, extracellular AAO has been reported in ligninolytic

Abbreviations
AAO, aryl-alcohol oxidase; FAD, flavin-adenine dinucleotide; GMC, glucose–methanol–choline.

basidiomycetes from the genera *Pleurotus*, *Bjerkandera* and *Trametes* [4–9]. The fungi from the two former genera also synthesize aromatic metabolites, such as *p*-anisaldehyde (4-methoxybenzaldehyde) and chlorinated *p*-anisaldehyde [10,11]. It has been demonstrated that these are the substrates for continuous production of hydrogen peroxide required for ligninolysis by redox cycling involving AAO and aryl-alcohol dehydrogenase [12]. In addition to acting as the oxidizing substrate for peroxidases, hydrogen peroxide also generates active oxygen species involved in the initial steps of fungal attack of the plant cell wall [13].

Whereas glyoxal oxidase is a protein radical–copper enzyme [14], both pyranose-2-oxidase and AAO are flavoenzymes [9,15]. AAO from *Pleurotus eryngii* is a monomeric glycoprotein of 70 kDa with dissociable flavin-adenine dinucleotide (FAD) as cofactor that catalyzes the oxidation of a variety of aromatic and aliphatic polyunsaturated alcohols to their corresponding aldehydes, using molecular oxygen as electron acceptor with concomitant production of hydrogen peroxide (Fig. 1). The gene coding for *P. eryngii* AAO was cloned [16] and expressed in *Emericella nidulans* (conidial state *Aspergillus nidulans*) [17]; the recombinant enzyme biochemical properties were similar to those of nonrecombinant AAO. Conditions for the crystallization of AAO purified from *Pleurotus* cultures have been reported [18], but a crystal structure for this enzyme has not been published yet, probably because of glycosylation microheterogeneity. Therefore, a molecular model of AAO from *P. eryngii* was obtained by homology modelling [19]. In the present study, molecular docking on the above model, site-directed mutagenesis and kinetic studies were used to identify the enzyme active site and evaluate the role of some selected residues in the catalytic mechanism of this flavooxidase.

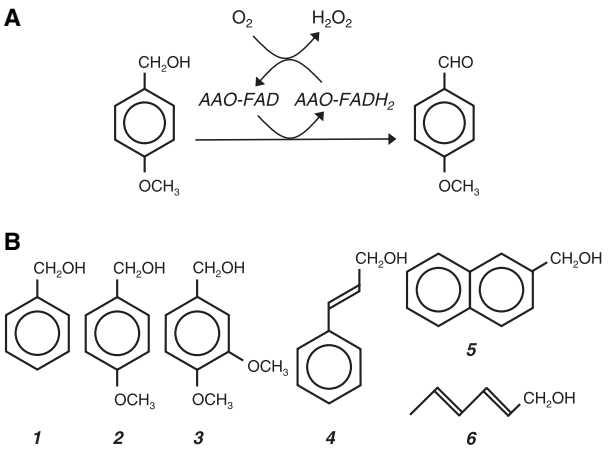

Fig. 1. AAO catalytic cycle (A) and substrates used in molecular docking calculations (B), including benzyl alcohol (1), *p*-anisyl alcohol (2), veratryl alcohol (3), cinnamyl alcohol (4), 2-naphthalenemethanol (5) and 2,4-hexadien-1-ol (6).

Results

Molecular docking of AAO substrates

A molecular model for *P. eryngii* AAO, built using the *Aspergillus niger* glucose oxidase crystal structure as template [19], was used to localize the active site (substrate-binding pocket) of AAO by molecular docking. The enzyme consists of two domains, the FAD-binding domain (bottom part) and the substrate-binding domain (top part), and one cofactor molecule with the adenine moiety buried in the FAD domain, and the flavin moiety expanding to the substrate domain (Fig. 2A).

Six AAO substrates with different molecular structures – benzyl, *p*-anisyl (4-methoxybenzyl), veratryl (3,4-dimethoxybenzyl) and cinnamyl alcohols, 2,4-hexadien-1-ol, and 2-naphthalenemethanol (Fig. 1B) – were separately docked on AAO. Ten substrate molecules were found after each docking calculation, and in all cases more than 50% of them clustered together in front of the *rectus* (*re*)-face of the isoalloxazine ring of the FAD cofactor. This substrate location is shown in Fig. 2A, which includes the 10 molecules of veratryl alcohol clustering together after docking. The putative substrate-binding pocket is connected to the protein surface by a main channel providing direct access to the *re*-side of the isoalloxazine ring, near two histidine side chains (Fig. 2B). Some 2-naphthalenemethanol and 2,4-hexadien-1-ol molecules docked at the *sinister* (*si*)-side of the flavin ring, but the corresponding cavity is some distance from FAD, and connected to the surface by a long channel. Inspection of the amino acid residues located around the putative substrate-binding site suggested that several residues are potentially involved in substrate oxidation by AAO (Fig. 2C).

Evaluation of AAO active site variants

Six residues potentially involved in AAO catalysis were selected after substrate docking and modified by site-directed mutagenesis. The different mutations were introduced in the *aao* cDNA by PCR and confirmed by DNA sequencing. The mutated cDNAs containing their signal sequence could be expressed in *E. nidulans* (under control of the inducible *alcA* promoter). The *aao* sequence was integrated into the *E. nidulans* genome as confirmed by PCR.

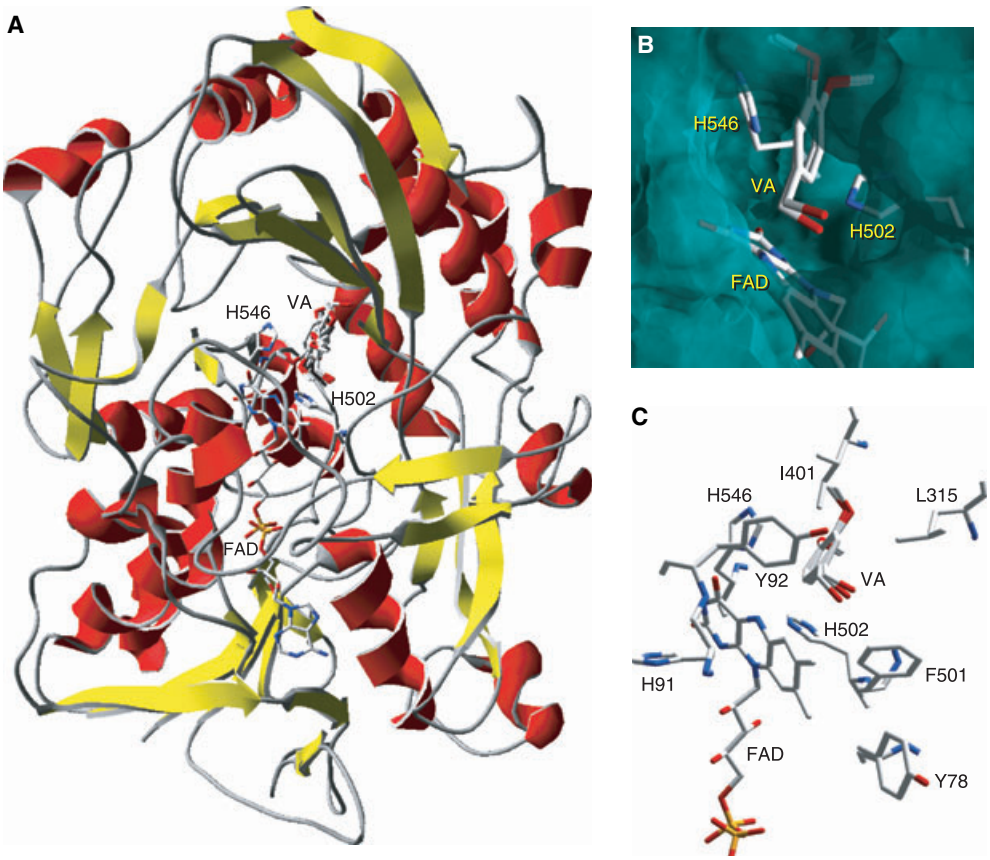

Fig. 2. AAO molecular model after veratryl alcohol docking. (A) General scheme of AAO molecular structure (Protein Data Bank entry 1QJN), showing secondary structure (predicted α-helices in red, and β-strands in yellow), FAD cofactor, two conserved histidine residues (His502 and His546), and 10 molecules of veratryl alcohol (VA). (B) Detail of solvent access surface, showing the entrance to the AAO active site cavity where veratryl alcohol was located after molecular docking. FAD cofactor (isoalloxazine ring), two conserved histidine residues (His502 and His546) and two VA molecules are shown. (C) Amino acid residues at the AAO active site, including those modified by site-directed mutagenesis. FAD cofactor (flavin moiety *si*-side) and two veratryl alcohol (VA) molecules after molecular docking are also shown.

E. nidulans transformants harbouring the *aao* sequence produced about 200 $U{\cdot}L^{-1}$ of wild-type AAO (approximately 2 $mg{\cdot}L^{-1}$) 56–74 h after induction. No AAO activity was detected in the nontransformed *E. nidulans* cultures. AAO was secreted by *E. nidulans*, and the activities of the site-directed variants (when active) could be directly detected in filtrates of 48 h cultures of the transformants harbouring the mutated *aao* sequences.

The first mutations introduced into AAO reduced the side chains of Tyr78, Tyr92, Leu315 and Phe501 to a methyl group. Other changes included introduction/removal of the phenolic hydroxyl in Tyr92 and Phe501, and substitution of His502 and His546 with leucine, serine and arginine residues. Only three of the variants obtained, Y78A (202 ± 28 $U{\cdot}L^{-1}$), Y92F (165 ± 45 $U{\cdot}L^{-1}$) and F501Y (215 ± 30 $U{\cdot}L^{-1}$), maintained activity levels in the same range of the wild-type enzyme (191 ± 19 $U{\cdot}L^{-1}$), using veratryl alcohol as substrate. Decreased activity was found for the L315A (16 ± 1 $U{\cdot}L^{-1}$) and F501A (4 ± 1 $U{\cdot}L^{-1}$) variants. All the other variants exhibited very low activity, such as H546R and H502R (1–2 ± 0 $U{\cdot}L^{-1}$), or null catalytic activity, such as Y92A, H502L, H502S, H546L and H546S (< 0.5 $U{\cdot}L^{-1}$), although AAO protein was produced, as evidenced by western blotting (data not shown). Although *E. nidulans* expression has the advantage of correct protein processing by the fungal host, limitations of the expression and purification protocols enabled the isolation of only those variants with some AAO activity.

Characterization of selected AAO variants

Five variants (Y78A, Y92F, L315A, F501A and F501Y) and wild-type AAO were purified to homogeneity

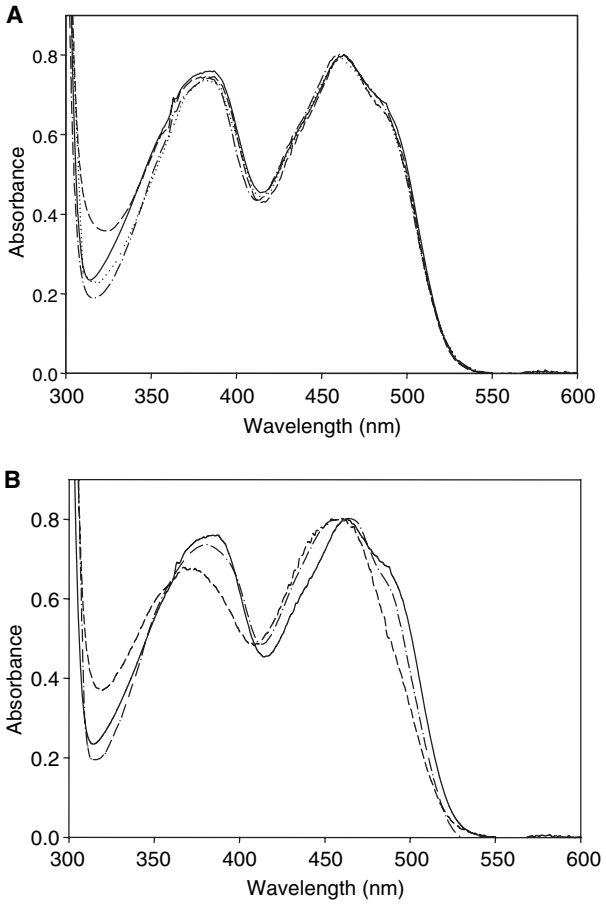

Fig. 3. Electronic absorption spectra of AAO variants. The spectra of wild-type AAO (continuous line) and site-directed variants were recorded in 10 mM sodium phosphate, pH 5.5 (at 78 μM AAO concentration). (A) Variants with similar spectra: Y78A (····), Y92F (- - - -) and F501Y (- · - ·). (B) Variants with differences in the spectra: L315A (- - - -) and F501A (- · - ·).

from recombinant *E. nidulans* cultures, with a final A_{280}/A_{463} ratio of about 10 in all cases. They showed a single band with an apparent molecular mass of 70 kDa after SDS/PAGE. The visible absorption spectra of the Y78A, Y92F and F501Y variants were very similar to that of wild-type AAO (Fig. 3A) with absorption maxima at 387 and 463 nm, indicating that the cofactor was in the oxidized state and correctly incorporated. The absorption maxima of L315A were situated at 372 and 459 nm, and the shoulder near 485 nm was not observed (Fig. 3B). The F501A variant also showed a shift of the second absorption maximum (situated around 460 nm) and decreased absorbance at 387 nm (Fig. 3B). These spectral shifts suggest that removal of the side chains of Leu315 and Phe501 increases the polarity of the flavin microenvironment.

Steady-state kinetic parameters of the five variants were determined for different alcohol substrates, and the corresponding values are shown in Table 1, compared with wild-type AAO produced also in *E. nidulans*. Most of the variants displayed lower catalytic efficiencies than wild-type AAO, although some of the differences were not significant, taking into account the standard deviations. However, no efficiency decrease, and even an increase with some substrates, was observed for the F501Y variant. This strongly contrasted with the results obtained when an aromatic side chain was absent in the F501A variant. This variant was 30–200-fold less efficient than wild-type AAO in oxidizing the different substrates, mainly due to a strong decrease in catalytic rate. The results obtained for Tyr92 were similar, as the activity was lost when an alanine residue was present (Y92A variant), and similar efficiencies were obtained when a tyrosine residue (wild-type AAO) or a phenylalanine residue (Y92F variant) was present. A third aromatic residue near the putative active site of AAO is Tyr78. However, the steady-state kinetic parameters of the Y78A variant showed that this residue is not required for catalytic activity, although some decrease in substrate (e.g. anisyl alcohol) oxidation was observed. Finally, the L315A variant showed decreased catalytic efficiency, which was especially evident on the best AAO substrates, such as *p*-anisyl alcohol (3.5-fold lower efficiency).

Discussion

AAO structure and active site

AAO has been recently included in the glucose–methanol–choline (GMC) oxidoreductase family [20]. This family, named after the initial members glucose oxidase, methanol oxidase and choline dehydrogenase [21], currently consists of more than 500 protein sequences. All of them show at least one of the two characteristic Prosite sequences (PS000623 and PS000624 motifs) and often an N-terminal consensus involved in FAD binding [22]. AAO shares the highest sequence identity (28% identity) with glucose oxidase from *A. niger* [23], and some hypothetical proteins such as choline dehydrogenase from *Vibrio vulnificus* (up to 34% identity) [24] (multiple alignment is provided in supplementary Fig. S1).

The AAO molecular model [19] has an FAD-binding domain formed by two main β-sheets and a variable number of α-helices, whose structure is conserved in the members of the GMC family whose structure has been solved [25–31], and a substrate-

Table 1. Steady-state kinetic constants of wild-type AAO and five AAO variants expressed in *Emericella nidulans* on different alcohols. Means and standard deviations of K_m (μM), k_{cat} (s^{-1}) and efficiency as k_{cat}/K_m (s^{-1}·mM^{-1}) from the normalized Michaelis–Menten equation after nonlinear fit of data (oxidation tests were carried out in 100 mM sodium phosphate, pH 6.0, at 24°C).

	Benzyl alcohol	*m*-Anisyl alcohol	*p*-Anisyl alcohol	Veratryl alcohol	2,4-Hexadien-1-ol
Wild-type					
K_m	632 ± 158	227 ± 105	27 ± 4	540 ± 27	94 ± 5
k_{cat}	30 ± 2	15 ± 2	142 ± 5	114 ± 2	119 ± 2
k_{cat}/K_m	47 ± 9	65 ± 24	5230 ± 615	210 ± 5	1270 ± 55
Y78A					
K_m	639 ± 68	293 ± 7	53 ± 1	492 ± 26	168 ± 17
k_{cat}	25 ± 1	8 ± 1	90 ± 2	83 ± 1	177 ± 5
k_{cat}/K_m	39 ± 3	28 ± 1	1700 ± 89	168 ± 7	1050 ± 87
Y92F					
K_m	985 ± 33	301 ± 6	39 ± 1	460 ± 12	113 ± 2
k_{cat}	33 ± 1	26 ± 1	139 ± 1	116 ± 2	206 ± 2
k_{cat}/K_m	33 ± 1	85 ± 2	3530 ± 105	253 ± 5	1830 ± 29
L315A					
K_m	719 ± 34	211 ± 10	40 ± 1	844 ± 30	114 ± 20
k_{cat}	19 ± 1	12 ± 1	60 ± 1	76 ± 1	56 ± 2
k_{cat}/K_m	26 ± 1	59 ± 2	1490 ± 44	89 ± 3	492 ± 74
F501A					
K_m	2550 ± 172	734 ± 27	26 ± 1	380 ± 35	263 ± 26
k_{cat}	1 ± 0	1 ± 0	3 ± 0	3 ± 0	1 ± 0
k_{cat}/K_m	0 ± 0	1 ± 0	102 ± 2	7 ± 1	6 ± 1
F501Y					
K_m	614 ± 37	215 ± 18	15 ± 1	317 ± 21	81 ± 6
k_{cat}	27 ± 1	17 ± 1	111 ± 2	86 ± 1	110 ± 2
k_{cat}/K_m	45 ± 2	78 ± 6	7660 ± 419	271 ± 15	1370 ± 86

binding domain including a large β-sheet and several α-helices, whose general structure and architecture of the catalytic site is more variable, in agreement with the different types of substrate of GMC oxidoreductases [21,32].

Molecular docking for localizing the substrate-binding pocket included six different polyunsaturated primary alcohols with the hydroxyl group in Cα, representative of the range of AAO substrates [9,19,33]. Most of these alcohols docked in front of the *re*-side of the isoalloxazine ring of FAD [34], with the benzylic carbon at 3.9 Å from its N5. The most frequently encountered substrate orientation was similar to that found in the crystal structure of the cholesterol oxidase–dehydroisoandrosterone complex [35]. After docking, six residues potentially involved in AAO catalysis, Tyr78, Tyr92, Leu315, Phe501, His502 and His546, were investigated by site-directed mutagenesis. The roles of the above aromatic and histidine residues are discussed below. Moreover, the lower k_{cat} and the modified spectrum of the Leu315 variant compared with wild-type AAO suggested that this residue affects the FAD environment, even without being located in the near vicinity of the cofactor, but further studies are required.

Conserved histidines at the AAO active site

AAO His502 is fully conserved in the sequences of the best-known GMC oxidoreductases, including glucose oxidase [23,32], cholesterol oxidase [36,37], choline oxidase [38], hydroxynitrile lyase [31] and the flavin domain of cellobiose dehydrogenase [39], whereas His546 is conserved in glucose oxidase and hydroxynitrile lyase, but replaced by asparagine in choline oxidase, the flavin domain of cellobiose dehydrogenase and cholesterol oxidase. The positions of the conserved histidine and histidine/asparagine residues near the FAD isoalloxazine ring of four of the above GMC oxidoreductases are shown in Fig. 4. Spatial conservation of these residues suggests a similar mechanism of substrate activation during catalysis. The current consensus mechanism for most GMC oxidoreductases involves removal of the substrate hydroxyl proton (alkoxide formation) by an active site base contributing to the transfer of a hydride from the substrate α-carbon to the flavin cofactor [40–46].

Site-directed mutagenesis suggested that the conserved histidine residue in cellobiose dehydrogenase [47] and cholesterol oxidase [27] is the active site base involved in substrate oxidation, although other basic

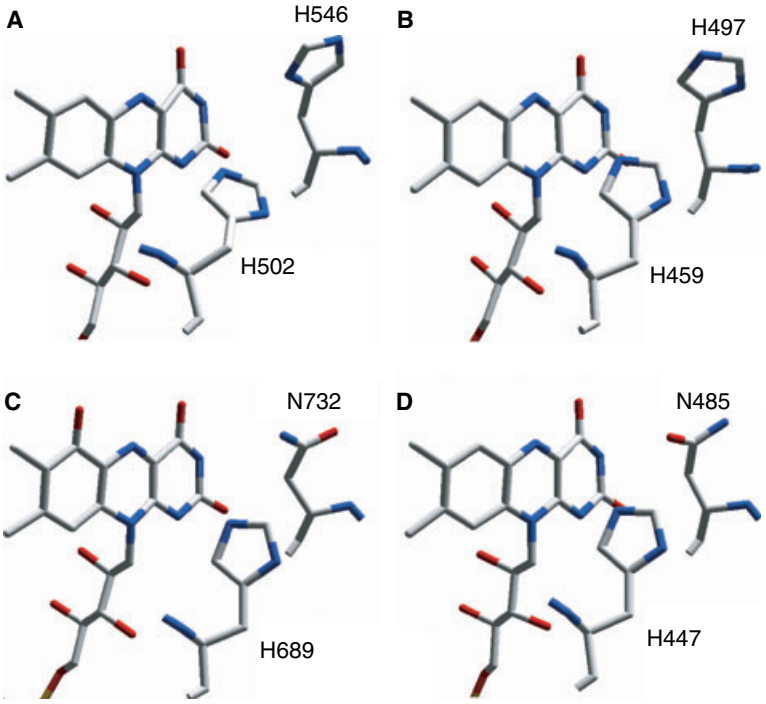

Fig. 4. Conserved residues at the active site of four GMC oxidoreductases. The positions of conserved histidine and histidine/asparagine at the *re*-side of the FAD isoalloxazine ring are shown. (A) AAO (Protein Data Bank entry 1QJN). (B) Hydroxynitrile lyase (Protein Data Bank entry 1JU2). (C) Cholesterol oxidase (Protein Data Bank entry 1COY). (D) Cellobiose dehydrogenase (Protein Data Bank entry 1KDG).

residues could play this role in the latter enzyme [28,48]. By contrast, in choline oxidase the conserved His466 (homologous to AAO His502) contributes to the stabilization of the substrate alkoxide formed by the action of an unidentified base [49,50]. His516 and His559 of glucose oxidase have been suggested as the active site base involved in catalysis [44,51]. In AAO, substitution of His502 and His546 with leucine and serine residues resulted in completely inactive variants, whereas some activity (although 100–200-fold lower) was detected when they were substituted with arginine, which could still contribute to the stabilization of a substrate alkoxide. As both histidine residues are equally required for AAO activity, and they are situated at similar distances from the hydroxyl of the docked substrate, they could cooperate in facilitating the hydride transfer from substrate to FAD. The decrease of activity of the AAO H502A and H546A variants (> 500-fold) is higher than found for the choline oxidase H466A variant (20-fold decrease) [49], supporting a direct role of these histidines in substrate activation by AAO. In the case of cholesterol oxidase, the H447A variant could not be expressed [52]; however, an activity decrease similar to that found in AAO was found for the H689A variant of cellobiose dehydrogenase [47].

Aromatic residues in the AAO active site

Several aromatic amino acid residues have been reported to be involved in binding of aromatic substrate by the flavoenzymes *p*-hydroxybenzoate hydroxylase (Tyr201, Tyr222 and Tyr385) [53], D-amino acid oxidase (Tyr55, Tyr224 and Tyr228) [54], and vanillyl-alcohol oxidase (Tyr108, Tyr187, Phe424 and Tyr503) [55]. The last of these is related to AAO, because it also oxidizes aromatic alcohols, but vanillyl-alcohol oxidase oxidizes phenolic benzylic alcohols, whereas the AAO substrates are nonphenolic alcohols.

Three aromatic amino acid residues located in the putative substrate-binding site of AAO were modified by site-directed mutagenesis. Tyr78 did not seem to be involved in catalysis, as the kinetic properties of the Y78A variant were not very different from those of wild-type AAO. This is in agreement with the AAO molecular model, where the Tyr78 side chain points away from the active site. However, removal of the aromatic side chain from either Tyr92 or Phe501 resulted in nearly complete loss of activity. By contrast, removing or introducing a side chain phenolic hydroxyl (Y92F and F501Y variants) did not reduce activity. This supports the view that these residues are not directly involved in substrate activation. In a similar way, the conserved Tyr223 at the active site of D-amino acid oxidase can be replaced by a phenylalanine residue without affecting activity [56]. Although a small decrease (3–4-fold) in the affinity of the F501A variant for most substrates was observed, the main effect of the mutation was a large decrease (20–80-fold) in catalytic rate. Simultaneously, a decrease in AAO redox potential of over 50 mV was found when Phe501 was

replaced by an alanine, suggesting that changes at this position can modulate the redox potential of the enzyme (F-D Munteanu, P Ferreira, FJ Ruiz-Dueñas, AT Martínez and A Cavaco-Paulo, unpublished results). These facts could be correlated with the modified electronic absorption spectrum of the F501A variant [47].

Interestingly, an aromatic residue homologous to AAO Phe501, contiguous with a fully conserved histidine, is present in most GMC oxidoreductase sequences (phenylalanine in AAO; tyrosine in *A. niger* glucose oxidase, cholesterol oxidase and choline dehydrogenase and oxidase; and tryptophan in *Penicillium amagasakiense* glucose oxidase, hydroxynitrile lyase and cellobiose dehydrogenase). No information on the role of this residue in other GMC oxidoreductases is available. In contrast, no aromatic residues at the position of AAO Tyr92 are present in any of the GMC oxidoreductase sequences mentioned above. However, inspection of the crystal structures revealed an aromatic residue from a different region of the glucose oxidase backbone (Tyr68) whose side chain occupies approximately the same position as that of AAO Tyr92 (Fig. 5). The involvement of this residue in glucose binding by glucose oxidase has been suggested after modelling [26].

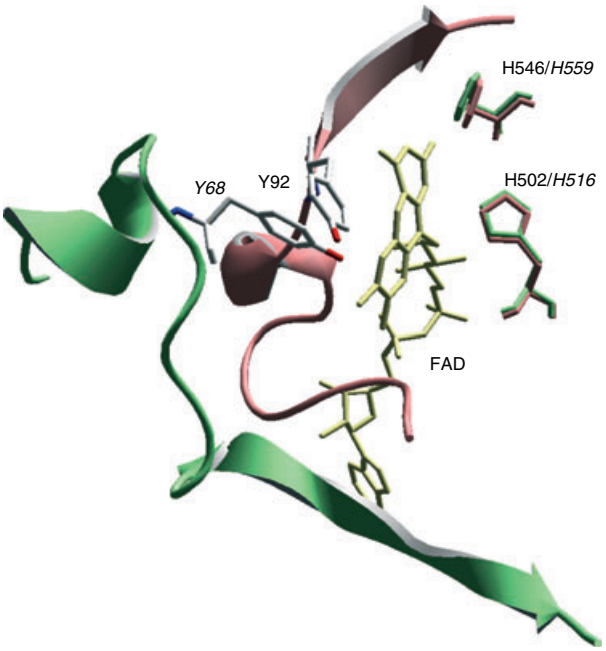

Fig. 5. AAO Tyr92 and glucose oxidase Tyr68 near FAD. Superposition of AAO (pink) and glucose oxidase (green), showing the similar position of side chains of two tyrosines (AAO Tyr92 and glucose oxidase Tyr68) from different backbone regions (*si*-side of the FAD isoalloxazine ring). FAD and conserved AAO His502 and His546, and glucose oxidase His516 and His559 (*re*-side of the FAD ring), are also shown (glucose oxidase residues in italics). From AAO and glucose oxidase 1GAL and 1QJN, respectively.

Moreover, site-directed mutagenesis of the homologous residue in the *Penicillium amagasakiense* glucose oxidase (Tyr73) confirmed its involvement in catalysis. However, a significant difference from AAO is that removal of the phenolic hydroxyl caused a 98% decrease in glucose oxidase catalytic efficiency [51], whereas activity is maintained in the Y92F AAO variant. It seems that Tyr92 in AAO is less essential for substrate binding than Tyr73 in glucose oxidase, perhaps because there is no need for a hydrogen bond interaction; however, the phenyl ring presence is critical.

Conclusions

The catalytic and spectral properties of AAO, an unusual oxidase of the GMC oxidoreductase family that does not thermodynamically stabilize an FAD semiquinone intermediate or form a sulphite adduct, have been recently described [33]. In the present study, the first evidence for the involvement of some amino acid residues in the catalytic activity of this enzyme has been obtained by site-directed mutagenesis after *in silico* docking. Two histidine residues (His502 and His546) in the vicinity of the flavin ring were found to be strictly required for AAO activity. One of these histidines is most likely involved in activation of the alcohol substrates by accepting the hydroxyl proton before hydride transfer to FAD, whereas the second one could be needed for binding and positioning of the substrate. Two aromatic residues (Tyr92 and Phe501) were also required for AAO activity, although this was not affected by the phenolic/nonphenolic nature of their aromatic side chains. An aromatic residue at position Phe501 of AAO is conserved in all GMC oxidoreductases, although its role has not been described. In AAO, comparison of the F501A and F501Y variants suggested that this residue could modulate the redox potential of the FAD, affecting the enzyme k_{cat} and electronic absorption spectrum, rather than being involved in substrate binding, as initially thought. These first AAO structure–function studies will be completed in the future to give us a better understanding of the catalytic mechanisms and biotechnological potential of an oxidase acting on unsaturated alcohols with very different molecular structures.

Experimental procedures

Chemicals

Benzyl, *m*-anisyl (3-methoxybenzyl), *p*-anisyl and veratryl alcohols, and 2,4-hexadien-1-ol, were obtained from Sigma-Aldrich (St Louis, MO, USA).

Fungal strains and plasmids

cDNA encoding *P. eryngii* AAO with its own signal peptide was cloned into plasmid *palc*A, and the resulting vector (pALAAO) was used for site-directed mutagenesis, and transformation of *E. nidulans bi*A1, *met*G1, *arg*B2 (IJFM A729), as described below [17].

Site-directed mutagenesis

AAO variants were obtained by PCR with the Quikchange site-directed mutagenesis kit from Stratagene (La Jolla, CA, USA), using the plasmid pALAAO as template, the primers including mutations (underlined) at the corresponding triplets (bold) (only direct constructions are shown) (Table 2).

Expression and purification of wild-type enzyme and AAO variants

Protoplasts of *E. nidulans* (*arg*B$^-$ strain) were prepared, and transformed with the pALAAO plasmids containing the different mutations; the transformants were then screened for arginine prototrophy [17]. Integration of the AAO cDNA into the *E. nidulans* genome was confirmed by PCR. Wild-type AAO and the different site-directed variants were produced in *E. nidulans* cultures (28 °C and 180 r.p.m.) grown in threonine medium, after 24 h of growth in minimal medium [17]. The time course of extracellular AAO activity was followed for 72 h after threonine induction. Secretion of AAO protein was confirmed by western blotting. For this, protein SDS/PAGE was run, and bands were transferred to nitrocellulose membranes, and incubated overnight with antibody to AAO [57]; AAO was then detected with the ECLT chemiluminescence system (Amersham, Uppsala, Sweden). Site-directed mutagenesis variants and wild-type AAO were purified from the induction medium after 48 h. Purification included Sephacryl S-200 and MonoQ chromatography following the procedure developed for AAO from *P. eryngii* cultures [9], that was then applied to recombinant AAO from *E. nidulans* [17]. UV–visible spectra (see below) and SDS/PAGE in 7.5% gels were used to confirm the purity of the enzyme.

Table 2. Oligonucleotides used as primers for PCR site-directed mutagenesis.

Mutations	Primer sequences (5′- to 3′)
Y78A	GGTCGGTCAATTGCG**GCT**CCTCGCGGCCGTATG
Y92A	GGTCTAGCTCTGTTCAC**GCC**ATGGTCATGATGCG
Y92F	GGTCTAGCTCTGTTCAC**TTC**ATGGTCATGATGCG
L315A	CCGACCATTTG**GCC**CTTCCTGCTGCC
F501A	CGCCAACACGATT**GCC**CACCCAGTTGGAACGG
F501Y	GCCAACACGATTT**TAC**GACCAGTTGGAACGGC
H502L	GCCAACACGATTTTC**CTC**CCAGTTGGAACGGCC
H502S	GCCAACACGATTTTC**AGC**CCAGTTGGAACGGCC
H502R	GCCAACACGATTTTC**CGC**CCAGTTGGAACGGCCv
H546L	CCCTTCGCGCCCAACGCA**CTT**ACCCAAGGACCG
H546S	CCCTTCGCGCCCAACGCA**AGT**ACCCAAGGACCG
H546R	CCCTTCGCGCCCAACGCA**CGC**ACCCAAGGACCG

AAO activity and kinetics

AAO activity was measured spectrophotometrically by monitoring the oxidation of veratryl alcohol to veratraldehyde [9]. The reaction mixture contained 8 mM veratryl alcohol in air-saturated 100 mM sodium phosphate, pH 6.0. One activity unit is defined as the amount of enzyme converting 1 μmol of alcohol to aldehyde per minute at 24 °C.

Steady-state kinetics was studied at 24 °C in 100 mM sodium phosphate, pH 6.0. The rates of oxidation of benzyl, *m*-anisyl, *p*-anisyl and veratryl alcohols, and 2,4-hexadien-1-ol, were determined spectrophotometrically. Molar absorption coefficients of benzaldehyde (ε_{250} 13 800 $M^{-1}\cdot cm^{-1}$), *m*-anisaldehyde (ε_{314} 2540 $M^{-1}\cdot cm^{-1}$), *p*-anisaldehyde (ε_{285} 16 950 $M^{-1}\cdot cm^{-1}$) and veratraldehyde (ε_{310} 9300 $M^{-1}\cdot cm^{-1}$) were from Guillén *et al.* [9], and that of 2,4-hexadien-1-al (ε_{280} 30 140 $M^{-1}\cdot cm^{-1}$) was from Ferreira *et al.* [33]. No kinetic constants were determined for 2-naphthalenemethanol, due to low solubility. The nonlinear regression tool of the SIGMAPLOT (Systat Software Inc., Richmond, CA, USA) program was used to fit the steady-state kinetics data (three replicates) using Eqn (1) and Eqn (2):

$$f = \frac{AX}{K + X} \quad (1)$$

$$f = \frac{BX}{1 + BX/A} \quad (2)$$

where A is the maximal turnover rate (k_{cat}), X is the substrate concentration, K is the Michaelis constant (K_m), and B is the catalytic efficiency (k_{cat}/K_m). Mean and standard deviations were obtained from the normalized Michaelis–Menten equations.

AAO electronic absorption spectra

UV–visible spectra were recorded at 24 °C in 100 mM sodium phosphate (pH 6.0), using a Hewlett Packard (Loveland, CO, USA) 8453 spectrophotometer. The molar absorption of AAO-bound FAD, 10 280 $M^{-1}\cdot cm^{-1}$ at 463 nm [33], was used to estimate AAO concentrations.

Molecular docking and sequence alignment

Automated simulations were conducted with the program AUTODOCK 3.0 (Scrips Research Institute, La Jolla, CA, USA) [58] to dock benzyl, *p*-anisyl, veratryl and cinnamyl alcohols, 2,4-hexadien-1-ol and 2-naphthalenemethanol substrates on the AAO molecular model (Protein Data Bank

entry 1QJN) [19]. Polar hydrogen atoms were added to the molecular model according to the valence and isoelectric point of each residue. Two different methods of atomic partial charge assignment were used: Kollman charges were assigned to the protein, and Gasteiger charges to the ligands.

Acknowledgements

This research was supported by EU contracts QLK3-99-590 and FP6-2004-NMP-NI-4-02456, and the Spanish projects BIO2002-1166 and BIO2005-02224. We thank Mario García de Lacoba (CIB, Madrid) for help in molecular docking calculations, and Francisco Guillén (University of Alcalá, Madrid) for valuable comments. PF acknowledges a Fellowship of the Spanish MEC, and FJR-D acknowledges an I3P contract of the Spanish CSIC.

References

1 Kirk TK & Farrell RL (1987) Enzymatic 'combustion': the microbial degradation of lignin. *Annu Rev Microbiol* **41**, 465–505.
2 Kersten PJ & Kirk TK (1987) Involvement of a new enzyme, glyoxal oxidase, in extracellular H_2O_2 production by *Phanerochaete chrysosporium*. *J Bacteriol* **169**, 2195–2201.
3 Daniel G, Volc J & Kubatova E (1994) Pyranose oxidase, a major source of H_2O_2 during wood degradation by *Phanerochaete chrysosporium*, *Trametes versicolor*, and *Oudemansiella mucida*. *Appl Environ Microbiol* **60**, 2524–2532.
4 Farmer VC, Henderson MEK & Russell JD (1960) Aromatic-alcohol-oxidase activity in the growth medium of *Polystictus versicolor*. *Biochem J* **74**, 257–262.
5 Bourbonnais R & Paice MG (1988) Veratryl alcohol oxidases from the lignin degrading basidiomycete *Pleurotus sajor-caju*. *Biochem J* **255**, 445–450.
6 Guillén F, Martínez AT & Martínez MJ (1990) Production of hydrogen peroxide by aryl-alcohol oxidase from the ligninolytic fungus *Pleurotus eryngii*. *Appl Microbiol Biotechnol* **32**, 465–469.
7 Muheim A, Waldner R, Leisola MSA & Fiechter A (1990) An extracellular aryl-alcohol oxidase from the white-rot fungus *Bjerkandera adusta*. *Enzyme Microb Technol* **12**, 204–209.
8 Sannia G, Limongi P, Cocca E, Buonocore F, Nitti G & Giardina P (1991) Purification and characterization of a veratryl alcohol oxidase enzyme from the lignin degrading basidiomycete *Pleurotus ostreatus*. *Biochim Biophys Acta* **1073**, 114–119.
9 Guillén F, Martínez AT & Martínez MJ (1992) Substrate specificity and properties of the aryl-alcohol oxidase from the ligninolytic fungus *Pleurotus eryngii*. *Eur J Biochem* **209**, 603–611.
10 Gutiérrez A, Caramelo L, Prieto A, Martínez MJ & Martínez AT (1994) Anisaldehyde production and aryl-alcohol oxidase and dehydrogenase activities in ligninolytic fungi from the genus *Pleurotus*. *Appl Environ Microbiol* **60**, 1783–1788.
11 de Jong E, Field JA, Dings JAFM, Wijnberg JBPA & de Bont JAM (1992) De novo biosynthesis of chlorinated aromatics by the white-rot fungus *Bjerkandera* sp. BOS55. Formation of 3-chloro-anisaldehyde from glucose. *FEBS Lett* **305**, 220–224.
12 Guillén F & Evans CS (1994) Anisaldehyde and veratraldehyde acting as redox cycling agents for H_2O_2 production by *Pleurotus eryngii*. *Appl Environ Microbiol* **60**, 2811–2817.
13 Guillén F, Gómez-Toribio V, Martínez MJ & Martínez AT (2000) Production of hydroxyl radical by the synergistic action of fungal laccase and aryl alcohol oxidase. *Arch Biochem Biophys* **383**, 142–147.
14 Whittaker MM, Kersten PJ, Nakamura N, Sanders-Loehr J, Schweizer ES & Whittaker JW (1996) Glyoxal oxidase from *Phanerochaete chrysosporium* is a new radical-copper oxidase. *J Biol Chem* **271**, 681–687.
15 de Koker TH, Mozuch MD, Cullen D, Gaskell J & Kersten PJ (2004) Isolation and purification of pyranose 2-oxidase from *Phanerochaete chrysosporium* and characterization of gene structure and regulation. *Appl Environ Microbiol* **70**, 5794–5800.
16 Varela E, Martínez AT & Martínez MJ (1999) Molecular cloning of aryl-alcohol oxidase from *Pleurotus eryngii*, an enzyme involved in lignin degradation. *Biochem J* **341**, 113–117.
17 Varela E, Guillén F, Martínez AT & Martínez MJ (2001) Expression of *Pleurotus eryngii* aryl-alcohol oxidase in *Aspergillus nidulans*: purification and characterization of the recombinant enzyme. *Biochim Biophys Acta* **1546**, 107–113.
18 Varela E, Böckle B, Romero A, Martínez AT & Martínez MJ (2000) Biochemical characterization, cDNA cloning and protein crystallization of aryl-alcohol oxidase from *Pleurotus pulmonarius*. *Biochim Biophys Acta* **1476**, 129–138.
19 Varela E, Martínez MJ & Martínez AT (2000) Aryl-alcohol oxidase protein sequence: a comparison with glucose oxidase and other FAD oxidoreductases. *Biochim Biophys Acta* **1481**, 202–208.
20 Albrecht M & Lengauer T (2003) Pyranose oxidase identified as a member of the GMC oxidoreductase family. *Bioinformatics* **19**, 1216–1220.
21 Cavener DR (1992) GMC oxidoreductases. A newly defined family of homologous proteins with diverse catalytic activities. *J Mol Biol* **223**, 811–814.

22 Wierenga RK, Terpstra P & Hol WGL (1986) Prediction of the ocurrence of the ADP-binding βαβ-fold in proteins, using an amino acid sequence fingerprint. *J Mol Biol* **187**, 101–107.
23 Frederick KR, Tung J, Emerick RS, Masiarz F, Chamberlain SH, Vasavada A, Rosenberg S, Chakraborty S, Schopter LM & Massey V (1990) Glucose oxidase from *Aspergillus niger*. Cloning, sequence, secretion from *Saccharomyces cerevisiae* and kinetic analysis of a yeast-derived enzyme. *J Biol Chem* **265**, 3793–3802.
24 Chen CY, Wu KM, Chang YC, Chang CH, Tsai HC, Liao TL, Liu YM, Chen HJ, Shen AB, Li JC *et al.* (2003) Comparative genome analysis of *Vibrio vulnificus*, a marine pathogen. *Genome Res* **13**, 2577–2587.
25 Hecht HJ, Kalisz HM, Hendle J, Schmid RD & Schomburg D (1993) Crystal structure of glucose oxidase from *Aspergillus niger* refined at 2.3 Å resolution. *J Mol Biol* **229**, 153–172.
26 Wohlfahrt G, Witt S, Hendle J, Schomburg D, Kalisz HM & Hecht H-J (1999) 1.8 and 1.9 Å resolution structures of the *Penicillium amagasekiense* and *Aspergillus niger* glucose oxidase as a basis for modelling substrate complexes. *Acta Crystallogr D Biol Crystallogr* **55**, 969–977.
27 Yue QK, Kass IJ, Sampson NS & Vrielink A (1999) Crystal structure determination of cholesterol oxidase from *Streptomyces* and structural characterization of key active site mutants. *Biochemistry* **38**, 4277–4286.
28 Lario PI, Sampson N & Vrielink A (2003) Sub-atomic resolution crystal structure of cholesterol oxidase: what atomic resolution crystallography reveals about enzyme mechanism and the role of the FAD cofactor in redox activity. *J Mol Biol* **326**, 1635–1650.
29 Vrielink A, Lloyd LF & Blow DM (1991) Crystal structure of cholesterol oxidase from *Brevibacterium sterolicum* refined at 1.8 Å resolution. *J Mol Biol* **219**, 533–554.
30 Hallberg BM, Henriksson G, Pettersson G & Divne C (2002) Crystal structure of the flavoprotein domain of the extracellular flavocytochrome cellobiose dehydrogenase. *J Mol Biol* **315**, 421–434.
31 Dreveny I, Gruber K, Glieder A, Thompson A & Krastky C (2001) The hydroxynitrile lyase from almond: a lyase that looks like an oxidoreductase. *Structure* **9**, 803–815.
32 Kiess M, Hecht HJ & Kalisz HM (1998) Glucose oxidase from *Penicillium amagasakiense*. Primary structure and comparison with other glucose-methanol-choline (GMC) oxidoreductases. *Eur J Biochem* **252**, 90–99.
33 Ferreira P, Medina M, Guillén F, Martínez MJ, van Berkel WJH & Martínez AT (2005) Spectral and catalytic properties of aryl-alcohol oxidase, a fungal flavoenzyme acting on polyunsaturated alcohols. *Biochem J* **389**, 731–738.
34 Fraaije MW & Mattevi A (2000) Flavoenzymes: diverse catalysts with recurrent features. *Trends Biochem Sci* **25**, 126–132.
35 Li J, Vrielink A, Brick P & Blow DM (1993) Crystal structure of cholesterol oxidase complexed with a steroid substrate: implications for flavin adenine dinucleotide dependent alcohol oxidases. *Biochemistry* **32**, 11507–11515.
36 Ishizaki T, Hirayama N, Shinkawa H, Nimi O & Murooka Y (1989) Nucleotide sequence of the gene for cholesterol oxidase from a *Streptomyces* sp. *J Bacteriol* **171**, 596–601.
37 Ohta T, Fujishiro K, Yamaguchi K, Tamura Y, Aisaka K, Uwajima T & Hasegawa M (1991) Sequence of gene *choB* encoding cholesterol oxidase of *Brevibacterium sterolicum*: comparison with *choA* of *Streptomyces* sp. SA-COO. *Gene* **103**, 93–96.
38 Fan F, Ghanem M & Gadda G (2004) Cloning, sequence analysis, and purification of choline oxidase from *Arthrobacter globiformis*: a bacterial enzyme involved in osmotic stress tolerance. *Arch Biochem Biophys* **421**, 149–158.
39 Li B, Nagalla SR & Renganathan V (1996) Cloning of a cDNA encoding cellobiose dehydrogenase, a hemoflavoenzyme from *Phanerochaete chrysosporium*. *Appl Environ Microbiol* **62**, 1329–1335.
40 Fan F & Gadda G (2005) On the catalytic mechanism of choline oxidase. *J Am Chem Soc* **127**, 2067–2074.
41 Hallberg BM, Henriksson G, Pettersson G, Vasella A & Divne C (2003) Mechanism of the reductive half-reaction in cellobiose dehydrogenase. *J Biol Chem* **278**, 7160–7166.
42 Menon V, Hsieh CT & Fitzpatrick PF (1995) Substituted alcohols as mechanistic probes of alcohol oxidase. *Bioorg Chem* **23**, 42–53.
43 Ortiz-Maldonado M, Entsch B & Ballou DP (2003) Conformational changes combined with charge–transfer interactions are essential for reduction in catalysis by *p*-hydroxybenzoate hydroxylase. *Biochemistry* **42**, 11234–11242.
44 Wohlfahrt G, Trivic S, Zeremski J, Pericin D & Leskovac V (2004) The chemical mechanism of action of glucose oxidase from *Aspergillus niger*. *Mol Cell Biochem* **260**, 69–83.
45 Gibson QH, Swoboda BE & Massey V (1964) Kinetics and mechanism of action of glucose oxidase. *J Biol Chem* **239**, 3927–3934.
46 Weibel MK & Bright HJ (1971) The glucose oxidase mechanism. Interpretation of the pH dependence. *J Biol Chem* **246**, 2734–2744.
47 Rotsaert FAJ, Renganathan V & Gold MH (2003) Role of the flavin domain residues, His689 and Asn732, in the catalytic mechanism of cellobiose dehydrogenase from *Phanerochaete chrysosporium*. *Biochemistry* **42**, 4049–4056.

48 Yin Y, Liu P, Anderson RG & Sampson NS (2002) Construction of a catalytically inactive cholesterol oxidase mutant: investigation of the interplay between active site-residues glutamate 361 and histidine 447. *Arch Biochem Biophys* **402**, 235–242.
49 Ghanem M & Gadda G (2005) On the catalytic role of the conserved active site residue His466 of choline oxidase. *Biochemistry* **44**, 893–904.
50 Ghanem M & Gadda G (2006) Effects of reversing the protein positive charge in the proximity of the flavin N(1) locus of choline oxidase. *Biochemistry* **45**, 3437–3447.
51 Witt S, Wohlfahrt G, Schomburg D, Hecht HJ & Kalisz HM (2000) Conserved arginine-516 of *Penicillium amagasakiense* glucose oxidase is essential for the efficient binding of β-D-glucose. *Biochem J* **347**, 553–559.
52 Kass IJ & Sampson NS (1998) Evaluation of the role of His447 in the reaction catalyzed by cholesterol oxidase. *Biochemistry* **37**, 17990–18000.
53 Schreuder HA, Prick PA, Wierenga RK, Vriend G, Wilson KS, Hol WGL & Drenth J (1989) Crystal structure of the *p*-hydroxybenzoate hydroxylase–substrate complex refined at 1.9 Å resolution. Analysis of the enzyme–substrate and enzyme–product complexes. *J Mol Biol* **208**, 679–696.
54 Mattevi A, Vanoni MA, Todone F, Rizzi M, Teplyakov A, Coda A, Bolognesi M & Curti B (1996) Crystal structure of D-amino acid oxidase: a case of active site mirror-image convergent evolution with flavocytochrome b2. *Proc Natl Acad Sci USA* **93**, 7496–7501.
55 Mattevi A, Fraaije MW, Mozzarelli A, Olivi L, Coda A & van Berkel WJH (1997) Crystal structures and inhibitor binding in the octameric flavoenzyme vanillyl-alcohol oxidase: the shape of the active-site cavity controls substrate specificity. *Structure* **5**, 907–920.
56 Harris CM, Molla G, Pilone MS & Pollegioni L (1999) Studies on the reaction mechanism of *Rhodotorula gracilis* D-amino-acid oxidase. Role of the highly conserved Tyr-223 on substrate binding and catalysis. *J Biol Chem* **274**, 36233–36240.
57 Barrasa JM, Gutiérrez A, Escaso V, Guillén F, Martínez MJ & Martínez AT (1998) Electron and fluorescence microscopy of extracellular glucan and aryl-alcohol oxidase during wheat-straw degradation by *Pleurotus eryngii*. *Appl Environ Microbiol* **64**, 325–332.
58 Morris GM, Goodsell DS, Halliday RS, Huey R, Hart WE, Belew RK & Olson AJ (1998) Automated docking using Lamarckian genetic algorithm and an empirical binding free energy function. *J Comp Chem* **19**, 1639–1662.

Supplementary material

The following supplementary material is available online:

Fig. S1. Multiple alignment of aryl-alcohol oxidase and related proteins obtained with CLUSTALW (CLUSTALW, http://www.ebi.ac.uk/clustalw) and ordered by sequence identity (NCBI entries and identity percentages are provided).

This material is available as a part of the online article from http://www.blackwell-synergy.com

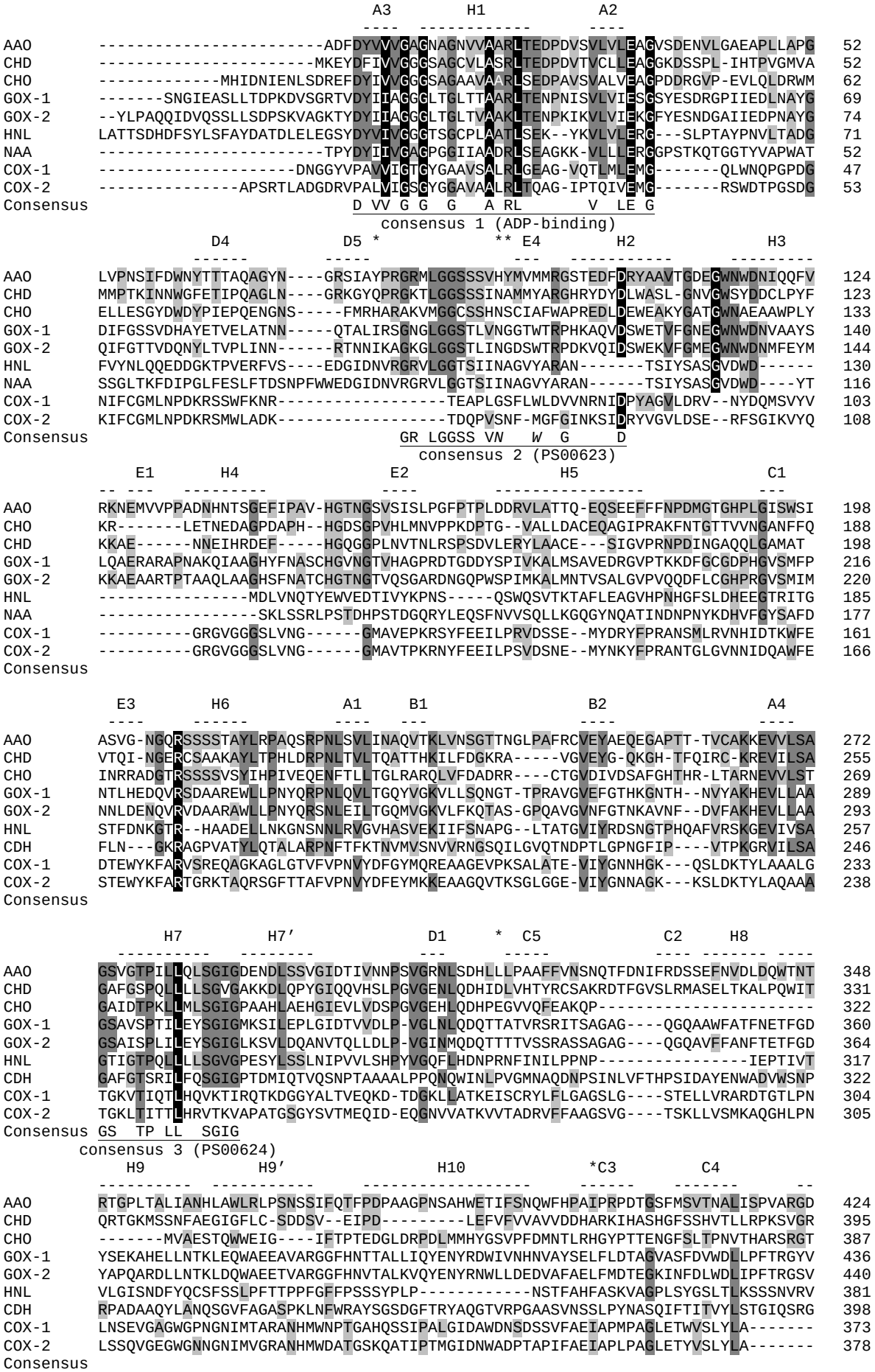
A3 H1 A2
consensus 1 (ADP-binding)
D4 D5 * ** E4 H2 H3
consensus 2 (PS00623)
E1 H4 E2 H5 C1
H7 H7′ D1 * C5 C2 H8
consensus 3 (PS00624)
H9 H9′ H10 *C3 C4
AAO
CHD
CHO
GOX-1
GOX-2
HNL
NAA
COX-1
COX-2
CDH
Consensus

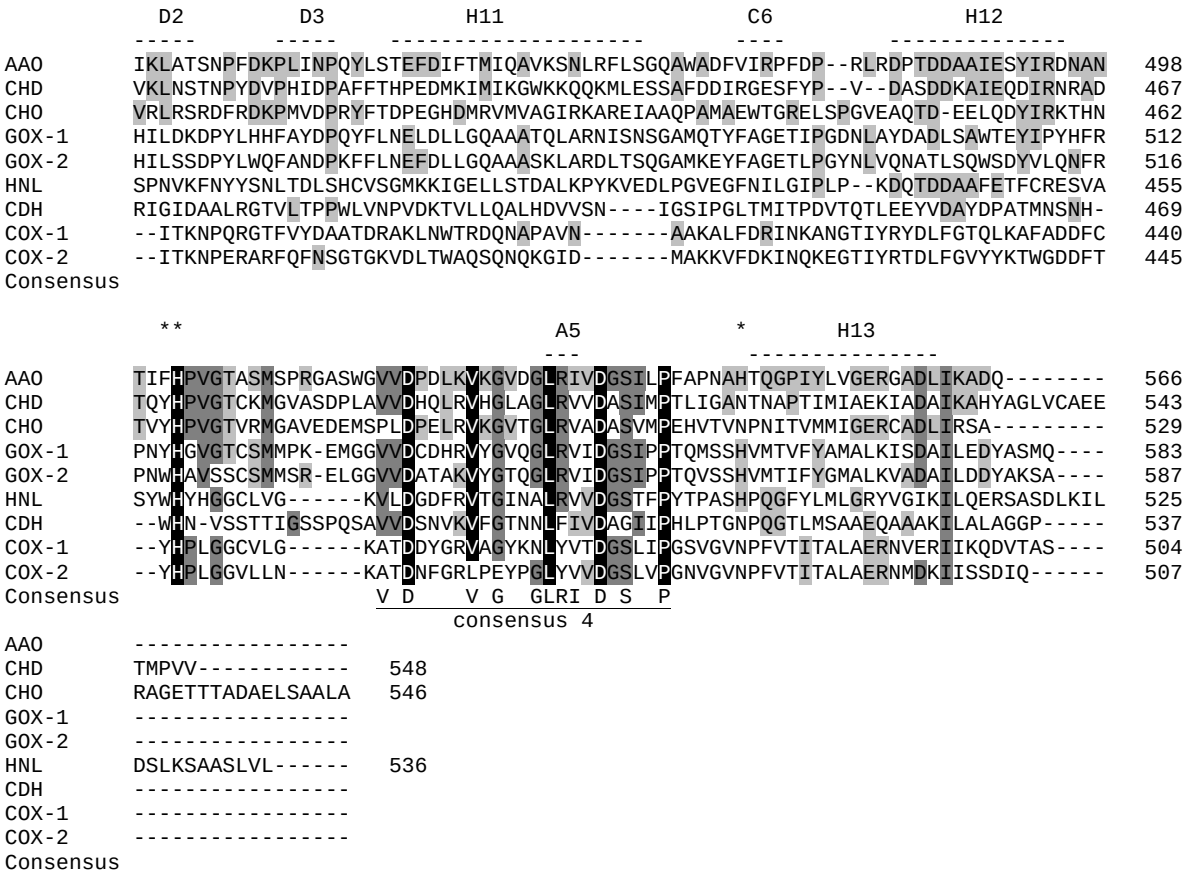

Fig. S1. Multiple alignment of AAO and related proteins obtained with ClustalW and ordered by sequence identity (NCBI entries, and identity percentages are provided): AAO, aryl-alcohol oxidase from *P. eryngii* (AAC72747); CHD, choline dehydrogenase from *V. vulnificus* (BAC95059; 34% identity); CHO, choline oxidase from *Arthrobacter globiformis* (AAP68832; 28% identity); GOX-1, glucose oxidase from *A. niger* (CAA34197; 28% identity); GOX-2, glucose oxidase from *P. amagasakiense* (AAD01493; 27% identity); HNL, hydroxynitrile lyase from *Prunus amygdalus* (O24243; 27% identity); CDH, flavin domain of cellobiose dehydrogenase from *P. chrysosporium* (Q01738; 23% identity); COX-1, cholesterol oxidase from *Streptomyces sp.* (P12676; 21% identity); and COX-2, cholesterol oxidase from *Brevibacterium sterolicum* (P22637; 21% identity). Residues have been highlighted as follows: black background, strictly conserved residues; gray background, conserved with respect to AAO sequence. Top line shows AAO secondary structure (α-helix and ß-strand, in sheets A to D, numbering being based on that of glucose oxidase) and the eight residues modified by site-directed mutagenesis (asterisks). Bottom line shows four sequences conserved in GMC family (AAO residues are indicated when the consensus includes several possibilities).